DFT-based Beamforming Weight-Vector Codebook Design for Spatially Correlated Channels in the Unitary Precoding Aided Multiuser Downlink

Du Yang, Lie-Liang Yang and Lajos Hanzo
School of ECS, University of Southampton, SO17 1BJ, UK
Tel: +44-23-8059 3364; Fax: +44-23-8059 4508
E-mail: dy05r,lly,lh@ecs.soton.ac.uk; http://www-mobile.ecs.soton.ac.uk

Abstract—The DFT-based beamforming weight-vector codebook is considered as an effective design for spatially correlated channels. In this paper, we demonstrate that when the antenna elements are uniformly spaced as well as linearly arranged, and the channels are spatially correlated, the codewords in a DFT-based beaforming weight-vector codebook approximately match the distribution of the optimal beamforming weight-vectors. As a result, the DFT-based codebook is indeed effective. Furthermore, we also demonstrate that if the antenna elements are uniformly spaced and circulary arranged, the statistical distribution of the optimal beamforming weight-vectors becomes different. We will demonstrate that in this scenario the DFT-based codebook will no longer outperform the Grassmannian codebook, which has not been shown in previous studies. Finally, an algorithm is proposed for constructing the DFT-based precoding matrix, which outperforms the conventional algorithm by ensuring the orthogonality of the precoding matrix.

Index Terms—DFT-based codebook, spatial correlated channel, unitary precoding, multiuser downlink

I. INTRODUCTION

In this paper, we employ the Unitary Precoding (UP) preprocessing scheme proposed for the Long-Term-Evolution (LTE) standard [1] in a multiuser DL system having multiple antenna aided Base Stations (BS) and single antenna aided Mobile Terminals (MTs). The Channel State Information (CSI) required by the UP scheme includes the knowledge of the unitary beamforming weight-vector and the channel quality. For a Frequency-Division-Duplex (FDD) system, where the Dowlink (DL) and the Uplink (UL) channels occupy different frequency bands and have different CSI, the most common way of acquiring CSI at the transmitter side is to estimate the CSI at the receiver, to quantise the estimated CSI using a predefined codebook and then to feed back the index of the chosen CSI codeword to the transmitter through a band-limited and potentially error-infected feedback channel. Hence, the design of the CSI quantization codebook is crucial for the success of any preprocessing technique. The quantizer design for the beamforming weight-vector is challenging because it is a multi-dimensional variable. Substantial research studies have been dedicated to this area and several solutions have been proposed [2]–[5]. The Grassmannian line-packing codebook

was proposed in [2] for a beamforming aided system communicating over spatially independent channels, while the Grassmannian subspace packing codebook was proposed in [4] for a spatial multiplexing assisted system. For spatially correlated channels, a modified Grassmannian-based codebook design was proposed in [5]. However, the LTE standard favours the Discrete Fourier Transform (DFT) based codebook proposed in [6], [7] for its simplicity, whose beamforming weight-vector codewords are actually permuted columns of a DFT matrix.

However, to the best of our knowledge, there is no study in the open literature on investigating the reason why the DFT-based codebook is effective for spatially correlated channels. The most detailed explanation we found in the open literature is in [8], where the author argued that the amplitude difference between the different antenna elements is reduced by spatially correlated fading, hence the constant-modulus DFT codebook imposes a lower CSI quantization error than the non-constant-modulus Grassmannian codebook. In this paper, we demonstrate that the DFT-based codebook hosts the Uniformly spaced and Linearly arranged Antenna Elements' (UL-AEs') Normalized Impulse Responses (NIRs) to a Single Resolvable Path (SRP). By exploiting the properties of this UL-AE NIR-SRP, a beneficial scheme is proposed for constructing an orthogonal DFT-based precoding matrix. Moreover, we demonstrate that for UL-AEs - provided that the channel is spatially correlated - the beamforming weight-vectors in a DFT-based codebook approximately match the distribution of the optimal beamforming weight-vectors. As a result, the DFT-based codebook is indeed effective. However, we will demonstrate that for Uniformly spaced and Circulary arranged Antenna Elements (UC-AEs), the statistical distribution of the optimal beamforming weight-vectors becomes different and hence the DFT-based codebook will no longer outperform the Grassmannian codebook, even for high spatial correlations. This problem has not been addressed in previous studies, where simplified statistical channel models were used.
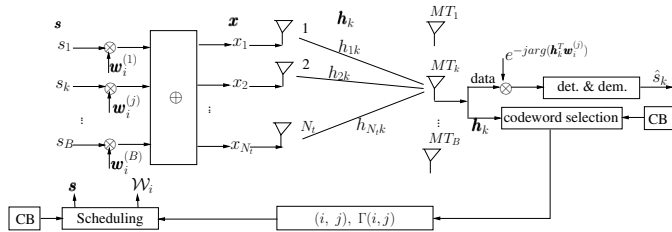
This paper is organised as follows. In Section II, the UP preprocessing scheme, the DFT-based beamforming weight-vector codebook and the UL-AE NIR-SRP are introduced. In Section III, the relationship between the beamforming weight-vector in a DFT-based codebook and the UL-AE NIR-SRP is presented, followed by the design of an algorithm for constructing an orthogonal precoding matrix. In Section IV, the

reasons behind the efficiency of the DFT-based beamforming weight-vector codebook designed for UL-AEs are highlighted, which are contrasted to its inefficiency for UC-AEs. Our simulation results are provided in Section V, followed by our conclusions.

II. PRELIMINARIES

A. The Unitary Precoding Aided Multi-User System

As illustrated in Fig. 1, a BS equipped with N_t downlink (DL) antennas communicates with K single-antenna aided MTs, which are uniformly dispersed over the cell. The wireless channels are assumed to be quasi-stationary flat Rayleigh fading, i.e. they have a constant envelope during each transmitted block. The simplifying assumption of perfect power control is used, hence no path-loss and shadowing are considered. It is also assumed that the total transmit power is equal to unity and that the noise variance N_0 is the same for all the K users. The beamforming weight-vector feedback channel is idealized, i.e. it is assumed to be both error-free and delay-free. The

CB: $\{\ \mathcal{W}_1 = [\boldsymbol{w}_1^{(1)}, \dots, \boldsymbol{w}_1^{(B)}];\ \dots ; \mathcal{W}_N = [\boldsymbol{w}_N^{(1)}, \dots, \boldsymbol{w}_N^{(B)}]\}, \boldsymbol{w}_i^{(j)} \in \mathcal{C}^{N_t \times 1}$

Fig. 1.   A multi-user system equipped with N_t transmit antennas at the BS and a single antenna at the MTs using the unitary precoding aided transmission scheme.

beamforming weight-vector codebook CB consisting of N precoding matrices $\mathcal{W}_i$, $i \in [1,\ N]$ is employed at both the BS and the MTs. Each precoding matrix $\mathcal{W}_i$ consists of B unitary precoding vectors $\boldsymbol{w}_i^{(j)}$, $\boldsymbol{w}_i^{(j)} \in \mathcal{C}^{N_t \times 1}$, $\boldsymbol{w}_i^{(j)^H} \boldsymbol{w}_i^{(j)} = 1$. In this study, we assumed that $B \leq N_t$, and the precoding vectors of a given precoding matrix are orthogonal to each other, i.e. we have $\boldsymbol{w}_i^{(j)^H} \boldsymbol{w}_i^{(k)} = 0$ for $B \geq 2$.

The kth MT first estimates its own Channel Impulse Response (CIR) $\boldsymbol{h}_k$ with the aid of the received pilot symbols, and then selects the preferred Precoding Matrix Index (PMI) i_k as well as the Precoding Vector Index (PVI) j_k from a pre-stored codebook CB, in order to maximise its own received SINR γ_k expressed as [1]

$$(i_k, j_k) = argmax_{1 \leq i \leq N, 1 \leq j \leq B} \gamma_k(i,j) \qquad (1)$$

$$= argmax_{1 \leq i \leq N, 1 \leq j \leq B} \frac{|\boldsymbol{h}_k^T \boldsymbol{w}_i^{(j)*}|^2}{B N_0 + \sum_{n \neq j} |\boldsymbol{h}_k^T \boldsymbol{w}_i^{(n)*}|^2},$$

where $(\cdot)^*$ represents the conjugate of a complex-valued scalar/vector/matrix. This selection criterion suggests that the MTs assume that all other beams in the precoding matrix $\mathcal{W}_i$-except for $\boldsymbol{w}_i^{(j)}$-will be scheduled for other users at an identical transmit power of $\frac{1}{B}$. Consequently, according to the

Shannon-Hartley law, the highest supportable rate of the kth user equals to $\Gamma_k(i_k, j_k) = log_2(1 + \gamma_k)$. In practice, Γ_k will be quantized using another codebook and fed back to the BS together with the above mentioned PMI and PVI. In this study, we assumed that using an arbitrary modulation and coding scheme is feasible in order to simplify our study. Having received the feedback information, the precoding matrix $\mathcal{W}_s$ and the associated intended users are selected with the aid of the following equation in order to maximise the achievable sum-rate of the B users

$$\mathcal{W}_s = \qquad (2)$$

$$argmax_{1 \leq i \leq N} \sum_{j=1}^{B} max_{1 \leq k \leq K} \Gamma_k(\gamma_k(i_k, j_k)) \delta(i - i_k, j - j_k),$$

where we have $\delta_k(i - i_k, j - j_k) = 1$ for $(i,j) = (i_k, j_k)$ and zero otherwise. The number of supported users is equal to B, when the number of active users K is sufficiently high, but it may be less than B, when K is small. Finally, the information signals of the B supported users are preprocessed by the precoding matrix $\mathcal{W}_s$ and they are transmitted simultaneously using the N_t transmit antennas.

B. DFT-based Beamforming Weight-Vector Codebook

The NB-by-NB DFT matrix $\boldsymbol{W}$ equals to [6]

$$\boldsymbol{W} = \frac{1}{\sqrt{NB}} \cdot \qquad (3)$$

$$\begin{bmatrix}
1 & 1 & 1 & \cdots & 1 \\
1 & e^{-j2\pi \cdot 1 \cdot \frac{1}{NB}} & e^{-j2\pi \cdot 1 \cdot \frac{2}{NB}} & \cdots & e^{-j2\pi \cdot 1 \cdot \frac{NB-1}{NB}} \\
1 & e^{-j2\pi \cdot 2 \cdot \frac{1}{NB}} & e^{-j2\pi \cdot 2 \cdot \frac{2}{NB}} & \cdots & e^{-j2\pi \cdot 2 \cdot \frac{NB-1}{NB}} \\
\vdots & \vdots & \vdots & \ddots & \vdots \\
1 & e^{-j2\pi \cdot (N_t-1) \cdot \frac{1}{NB}} & e^{-j2\pi \cdot (N_t-1) \cdot \frac{2}{NB}} & \cdots & e^{-j2\pi \cdot (N_t-1) \cdot \frac{NB-1}{NB}} \\
\vdots & \vdots & \vdots & \ddots & \vdots \\
1 & e^{-j2\pi \cdot (NB-1) \cdot \frac{1}{NB}} & e^{-j2\pi \cdot (NB-1) \cdot \frac{2}{NB}} & \cdots & e^{-j2\pi \cdot (NB-1) \cdot \frac{NB-1}{NB}}
\end{bmatrix}.$$

The first N_t rows of $\boldsymbol{W}$ with a normalization factor of $\frac{1}{\sqrt{N_t}}$ constitute the DFT-based beamforming weight-vector codebook, whose codeword $\boldsymbol{w}$ is expressed as

$$\boldsymbol{w}(l) = \frac{1}{\sqrt{N_t}} \begin{bmatrix} 1 & e^{-j2\pi \cdot 1 \cdot l} & e^{-j2\pi \cdot 2 \cdot l} & \cdots & e^{-j2\pi \cdot (N_t-1) \cdot l} \end{bmatrix}^T,$$
$$(4)$$

$$l = 0, \frac{1}{NB}, \frac{2}{NB}, \dots, \frac{NB-1}{NB}.$$

Moreover, for constructing precoding matrix, it is defined in [6] that the jth beamforming weight-vector in the ith precoding matrix $\boldsymbol{w}_i^{(j)}$ is calculated using Equation (4) by setting $l = \frac{j*N+i}{NB}$. However, the orthogonality of the constructed precoding matrix cannot be guaranteed using this algorithm.

C. UL-AE NIR-SRP

As illustrated in Fig. 2, the transmit AEs are arranged in a line with a spacing of $\Delta_t \lambda_c$, where Δ_t represents the distance between the adjacent antennas normalised by the wavelength λ_c of the carrier frequency. For a single resolvable path having an Angle of Departure (AOD) of θ, the CIR $\boldsymbol{h}_s$ is formulated as [9] $\boldsymbol{h}_s(\theta) =$
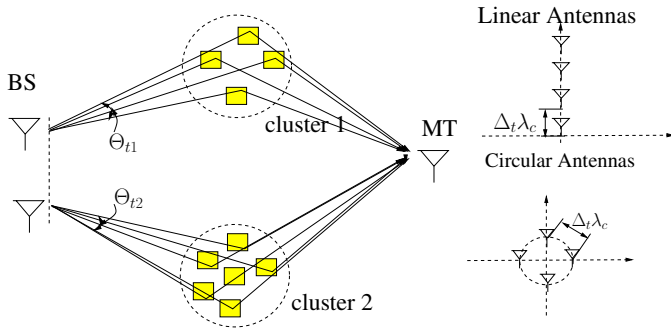
Fig. 2. Physical channel model for uniformly spaced linearly allocated antenna elements and uniformly spaced circularly allocated antenna elements.

$$ae^{j\phi} \begin{bmatrix} 1 & e^{-j2\pi \cdot 1 \cdot \Delta_t cos\theta} & \dots & e^{-j2\pi \cdot (N_t-1) \cdot \Delta_t cos\theta} \end{bmatrix}^T,$$

where a and ϕ represent the signal amplitude and the phase rotation, respectively. Hence, the UL-AEs' normalized impulse response to a single resolvable path is expressed as

$$\boldsymbol{e}_{UL-AEs}(\theta) = \frac{\boldsymbol{h}_s(\theta)}{||\boldsymbol{h}_s(\theta)||} \qquad (5)$$
$$= \frac{1}{\sqrt{N_t}} \begin{bmatrix} 1 & e^{-j2\pi \cdot 1 \cdot \Delta_t cos\theta} & \dots & e^{-j2\pi \cdot (N_t-1) \cdot \Delta_t cos\theta} \end{bmatrix}^T.$$

III. CONSTRUCTION OF AN ORTHOGONAL DFT-BASED PRECODING MATRIX RELYING ON THE RELATIONSHIP BETWEEN $\boldsymbol{w}_i^{(j)}$ AND $\boldsymbol{e}_{UL-AEs}$

By comparing Equations (4) and (5), it may be shown that if $l = \Delta_c cos\theta$, we have:

$$\boldsymbol{w}(l) = \frac{1}{\sqrt{N_t}} \begin{bmatrix} 1 & e^{-j2\pi l} & \dots & e^{-j2\pi(N_t-1)l} \end{bmatrix}^T \qquad (6)$$
$$= \frac{1}{\sqrt{N_t}} \begin{bmatrix} 1 & e^{-j2\pi(\Delta_t cos\theta)} & \dots & e^{-j2\pi(N_t-1)(\Delta_t cos\theta)} \end{bmatrix}^T$$
$$= \boldsymbol{e}_{UL-AEs}(\theta).$$

Hence, the beamforming weight-vectors in a DFT-based codebook host the UL-AE NIR-SRP. One of the important properties of $\boldsymbol{e}_{UL-AEs}$ stated in [9] is that the absolute value of its inner product $g_e = |\boldsymbol{e}_{UL-AEs}(\theta_1)^H \boldsymbol{e}_{UL-AEs}(\theta_2)|$ equals to $\left| \frac{sin(\pi N_t(\Delta_t cos\theta_1 - \Delta_t cos\theta_2))}{N_t sin(\pi(\Delta_t cos\theta_1 - \Delta_t cos\theta_2))} \right|$. Furthermore, $g_e = 0$ when we have $|cos\theta_1 - cos\theta_2| = \frac{k}{\Delta_t N_t}$, $k = 1, 2, \dots, N_t-1$. Physically, this implies that a beam steered to θ_1 will completely suppress any signal arriving from θ_2 as long as $|cos\theta_1 - cos\theta_2| = \frac{k}{\Delta_t N_t}$. By substituting $\Delta_t cos\theta$ for l, the sufficient condition of having two orthogonal beamforming weight-vectors $\boldsymbol{w}$ is obtained as follows:

If two beamforming weight-vectors in a DFT-based codebook $\boldsymbol{w}_1(l_1)$ and $\boldsymbol{w}_2(l_2)$, $l_1, l_2 \in [0, \frac{1}{NB}, \dots, \frac{NB-1}{NB}]$ are orthogonal to each other, then we have $|l_\Delta| \doteq |l_1 - l_2| = \frac{k}{N_t}, k = 1, \dots, N_t - 1$.

Consequently, an algorithm of constructing an orthogonal DFT-based precoding matrix is proposed and illustrated in Table I using Matlab code. The idea is to first calculate an appropriate periodic value $T \in \frac{1}{N_t}, \frac{2}{N_t}, \dots, \frac{N_t-1}{N_t}$, and then to assign the adjacent beamforming codewords of a given precoding matrix according to the relationship of $|x_i(j) - x_i^{(j+1)}| = T$. This algorithm is applicable for $B \leq N_t$. For

$N_t = nB, n \in \mathcal{N}$, the same codebook is generated by using this algorithm and by using the one proposed in [6] described in Section II-B, since they employ the same value of T.

TABLE I
THE IMPROVED DFT CODEBOOK GENERATION ALGORITHM

$T = floor(N_t/B)/N_t;$ %$floor(x) = \lfloor x \rfloor$
for $i = 1 : N$
$x = \frac{i-1}{NB};$
for $j = 1 : B$
$l = x + T * (j-1);$
$\boldsymbol{w}_i^{(j)} = \boldsymbol{w}(l);$ %$\boldsymbol{w}(x)$ is expressed in Equation (4)
end
end

IV. EFFICIENCY OF THE DFT-BASED BEAMFORMING WEIGHT-VECTOR CODEBOOK

Based on quantization theory, the DFT-based beamforming weight-vector codebook can be considered as an efficient design, if it assigns its quantization levels according to the statistical distribution of the optimal beamforming weight-vectors $\boldsymbol{w}_{opt}$ so as to minimize the quantization error [10]. Moreover, the optimal weight-vector $\boldsymbol{w}_{opt}$ in our study is equivalent to the normalised CIR $\boldsymbol{w}_{opt} = \frac{\boldsymbol{h}}{||\boldsymbol{h}||}$, which maximizes the receiver's SINR as well as the resultant sum-rate according to Equation (1). The statistical distribution of $\boldsymbol{w}_{opt}$ depends on the channel's properties, which are discussed as follows.

A. Spatially Correlated Channels Using UL-AEs

For full spatially correlated channels using UL-AEs, $\boldsymbol{w}_{opt}$ is equal to the UL-AE NIR-SRP. Using the physical channel model characterized in Fig. 2, the CIR $\boldsymbol{h}$ is formulated as $\boldsymbol{h} = \sum_j^J \sum_i^I \boldsymbol{h}_s = \sum_j^J \sum_i^I a_j^{(i)} e^{j\phi_j^{(i)}} \boldsymbol{e}_{UL-AEs}(\theta_j^{(i)})$, where I represents the number of resolvable paths in a cluster, while J denotes the number of clusters. The $\theta_j^{(i)}$ of each path AOD has a Gaussian distribution with a mean value of Θ_j and an angular spreading variance of σ_j. The spatial correlation ρ of the CIR $\boldsymbol{h}$ will increase when the number of paths, clusters and the angular spreading variance decrease. The channel exhibits full spatial correlation associated with $\rho = 1$ if $J = 1$, $I = 1$ and $\sigma_j = 0$. In this case, we have $\boldsymbol{w}_{opt} = \frac{\boldsymbol{h}}{||\boldsymbol{h}||} = \frac{\boldsymbol{h}_s}{||\boldsymbol{h}_s||} = \boldsymbol{e}_{UL-AEs}$.

Based on Equation (5), the vector $\boldsymbol{e}_{UL-AEs}$ can be represented as a function of a real-valued scalar variable x expressed as $\boldsymbol{e}_{UL-AEs}(x) = \frac{1}{\sqrt{N_t}} \begin{bmatrix} 1 & e^{-j2\pi \cdot 1 \cdot x} & \dots & e^{-j2\pi \cdot (N_t-1) \cdot x} \end{bmatrix}^T, x \doteq \Delta_t cos\theta$. Moreover, $\boldsymbol{e}_{UL-AEs}(x)$ is a periodic function with a period of $T = 1$ for $e^{-j2\pi \cdot k \cdot x} = e^{-j2\pi \cdot k \cdot (x+1)}$. By setting $\beta = mod(x, T), x = \Delta_t cos\theta, x \in [-\Delta_t, \Delta_t], T = 1, \beta \in [0, 1)$, a unique and unambiguous one-to-one relationship is constructed between the variable β and the vector $\boldsymbol{e}_{UL-AEs}$. As a result, we have the Probability Density Function (PDF) $p(\boldsymbol{e}_{UL-AEs}) = p([f(\beta)]) = p(\beta)$, where the original problem of finding the distribution of the optimal beamforming vectors $\boldsymbol{w}_{opt}$ becomes equivalent to that of identifying the distribution of the variable β.

Since the users are uniformly dispersed in a cell, we have $\theta \sim U(0, 2\pi), p(\theta) = \frac{1}{2\pi}$. Upon defining $\Omega \doteq cos\theta$, the PDF of Ω becomes equal to $p(\Omega) = \frac{1}{\pi\sqrt{1-\Omega^2}}$. The PDF of the

variable β recorded for $\Delta_t = 0.5$; $\Delta_t = 4$ and $\Delta_t = \frac{4}{3}$ using Monte-Claro simulation is shown in Fig. 3. In fact, the curve corresponding to $\Delta_t = 4$ respresents the shape of all PDFs, when we have $\Delta_t = k$, $k \in \mathcal{N}$. Fig. 3 demonstrates that except for a few high-density distribution peaks, β is near-uniformly distributed in the range of $[0, 1)$.

Equation (4) demonstrated that the beamforming weight-vector codewords in a DFT-based codebook are also uniformly distributed over $[0, 1)$, with samples at distances of $\frac{1}{NB}$. Hence, the DFT-based beamforming weight-vector codebook has a PDF reminiscent of the distribution of the optimal beamforming vector of a fully spatially correlated channel. Naturally, when the spatial correlation coefficient ρ decreases, the distribution of β becomes less similar to the distribution of the optimal beamforming vector. Consequently, the DFT-based codebook becomes less effective.

B. Spatially Correlated Channels Using UC-AEs

When N_t antennas are equally spaced around a circle with a distance of $\Delta_t \lambda_c$, the UC-AEs NIR-SRP is represented as $e_{UC-AEs}(\theta) = \frac{1}{\sqrt{N_t}} \left[e^{-j2\pi\Delta_R cos(\theta - \frac{2\pi}{N_t})} \quad \ldots \quad e^{-j2\pi\Delta_R cos(\theta - \frac{2\pi(N_t-1)}{N_t})} \right]^T$, where $\Delta_R = \frac{\Delta_t}{2sin(\frac{\pi}{N_t})}$ is the radius of the circle. Similarly, e_{UC-AEs} is the optimal beamforming weight-vector for fully spatially correlated channels using UC-AEs. However, its distribution cannot be modelled by that of the same scalar variable β, which is uniformly distributed betwen 0 and 1. As a result, the DFT-based beamforming weight-vector codebook does not represent an efficient design for the UC-AEs. The simulation results of Section V will demonstrate that the performance of the DFT-based codebook in fact becomes even worse than that of the Grassmannian codebook.

Unfortunately, the UC-AEs unit spatial signature e_{UC-AEs} cannot be expressed as a function of a scalar variable such as Δ_t, θ or any combination of Δ_t and θ. As a result, it is difficult to capture and characterize its distribution. However, we have observed in our informal investigations that for $\Delta_t = 0.5$ the beamwidth Φ is the same for any AOD. Hence, we proposed a quantization method, which uniformly samples the angular range of $\theta \in [0, 2\pi)$ with a displacement equal to $\frac{\Phi}{2k}, k = 1, 2, \ldots$. Consequently, any angular samples with an angular separation of $\frac{\Phi}{2}$ are orthogonal with respect to each other and can be used to construct orthogonal codebooks for $B = 2$. In practice, however, more sophisticated designs are needed for arbitrary values of Δ_t, B and N_t.

V. SIMULATION RESULTS

Fig. 4 demonstrates the achievable throughput gain of the improved DFT-based codebook generated by the algorithm summarised in Table I, as well as the achievable throughput of the conventional DFT-based beamforming weight-vector codebook generated according to Equation (4) at SNR=10dB, when the AEs are uniformly spaced and are arranged in a line. The throughput was calculated as $\sum_{k=1}^{B} log(1 + \gamma_k)$, where γ_k represents the SINR of the kth selected user defined in Equation (1) using the selection criterion stated in Equation (2). Four scenarios were considered, namely $N_t = 3, \rho = 1, B = 2, N = 8$; $N_t = 3, \rho = 0.12, B = 2, N = 8$; $N_t = 6, \rho = 1, B = 2, N = 8$ and $N_t = 6, \rho = 0.12, B = 4, N = 4$. Four feedback bits were used for all four scenarios, since the codebook-size was $NB = 16$. The following observations can be made based on the simulation results of Fig. 4. Firstly, the achievable sum-rate increases with the number of active users, as a benefit of the increased multi-user diversity. Secondly, if $N_t = nB, n \in \mathcal{N}$, for example, we have $N_t = 6, B = 2$, then the conventional scheme and the proposed scheme generate the same codebook, both representing orthogonal precoding matrices, hence the same performances are achieved. Thirdly, if $N_t \neq nB, n \in \mathcal{N}$, for example, we have $N_t = 3, B = 2$ and $N_t = 6, B = 4$. Then using the codebook generated by the proposed algorithm is capable of achieving a substantially higher throughput, since the inter-user interference is reduced, when using an orthogonal precoding matrix. Fourthly, the achievable throughput is significantly reduced, when the spatial correlation coefficient is $\rho = 0.12$ ($\Delta_t = 2, J = 6, I = 20, \sigma_j = 5$), because the DFT-based conventional codebook is less effective for channels exhibiting a low spatial correlation.

Fig. 5 compared the achievable sum-rate of the K users for both the DFT-based codebook and for the Grassmannian subspace packing codebook [4] at $SNR = 10dB$, and $N_t = 4$ using UL-AEs. When the channel is fully spatially correlated as indicated by $\rho = 1$, the achievable sum-rate of the K users employing the DFT-based codebook and $B = 2$, $N = 8$ is almost twice the achievable sum-rate of the Grassmannian subspace packing codebook having the same codebook size. By contrast, when the spatial correlation was decreased to $\rho = 0.21$ ($\Delta_t = 0.5, J = 6, I = 20, \sigma_j = 5$), the performance of the DFT-based codebook degraded, while that of the Grassmannian subspace packing codebook improved. When the channel became spatially independent, i.e. we had $\rho = 0$, the achievable rate of using the Grassmannian subspace packing codebook and the one using the DFT-based codebook associated with $NB = 16$ codewords was similar. However, when the codebook size increased to $B = 2, N = 64$, the achievable sum-rate of the K users employing the Grassmannian subspace packing codebook was about 2bits/symbol higher than that of the one using the DFT-based codebook having the same codebook size. Hence, the following conclusions may be obtained. Firstly, the DFT-based codebook having a small size constitutes an effective design for both spatially correlated and independent channels. Secondly, the Grassmannian-based codebook associated with a sufficiently large codebook size is an effective design alternative for spatially independent channels. Thirdly, more quantization bits are required for spatially independent channels, because the beamforming vectors are more dissimilar. Fig. 5 also demonstrates that the achievable sum-rate of spatially independent channels using the Grassmannian-based codebook having seven feedback bits is significantly lower than that of the fully spatially correlated channel using the DFT-based codebook having only four feedback bits. This indicates that a BS can either reduce the AE spacing to obtain an increased throughput or increase the AE spacing to achieve a diversity gain.

Fig. 6 illustrates the achievable sum-rate of the K users for the DFT-based codebook, the Grassmannian-based codebook and the proposed codebook described in Section IV-B at $SNR = 10dB, N_t = 4, \Delta_t = 0.5, B = 2, N = 8$, when the AEs are uniformly spaced and arranged in a circle. When the channel is fully spatially correlated, the achievable sum-rate using the DFT-based codebook becomes lower than that of the Grassmannian-based codebook. When using the proposed codebook, a substantial throughput gain is obtained. Hence, we conclude that the DFT-based codebook is ineffective for UC-AEs. When the spatial correlation was decreased to $\rho = 0.1227$, the achievable sum-rate of both the DFT-based codebook and of the Grassmannian codebook increased compared to the $\rho = 1$ scenario and their difference became subtle. This is because the beamforming vectors' distribution becomes more dispersed across the entire N_t-dimensional unit sphere. As a result, both the DFT-based and the Grassmannian-based codebooks become more effective.

VI. CONCLUSION

In this paper, we have analysed the DFT-based beam-forming weight-vector codebook employed in the unitary precoding aided multi-user downlink. By recognising the fact that the beamforming weight-vector in a DFT-based codebook is constituted by the UL-AE NIR-SRP, an algorithm was proposed for constructing the corresponding DFT-based orthogonal precoding matrix. It was demonstrated that the DFT-based codebook is effective for UL-AEs, but not for UC-AEs. The simulation results of Fig. 5 also demonstrated that for spatially independent channels the Grassmannian codebook will only outperform the DFT-based codebook, if the codebook size is sufficiently large.

REFERENCES

[1] S. Sesia, I. Toufik, and M. Baker, *LTE: The UMTS Long Term Evolution from Theory to Practice*. John Wiley and Sons Ltd, 2009.

[2] D. J. Love, R. W. Heath, and T. Strohmer, "Grassmannian beamforming for multiple-input multiple-output wireless systems," *IEEE Transactions on Information Theory*, vol. 49, no. 10, pp. 2735–2747, Oct. 2003.

[3] D. Yang, L. L. Yang, and L. Hanzo., "Performance of SDMA systems using transmitter preprocessing based on noisy feedback of vector-quantized channel impulse responses," in *Vehicular Technology Conference, 2007. VTC2007-Spring. IEEE 65th*, Dublin, Apr. 2007, pp. 2119–2123.

[4] D. J. Love and R. W. Heath, "Limited feedback unitary precoding for spatial multiplexing systems," *IEEE Transactions on Information Theory*, vol. 51, no. 8, pp. 2967–2976, Aug. 2005.

[5] V. Raghavan, R. W. Heath, and A. M. Sayeed, "Systematic codebook designs for quantized beamforming in correlated MIMO channels," *IEEE Journal on Selected Areas in Communications*, vol. 25, no. 7, pp. 1298–1310, Sept. 2007.

[6] "Results on zero-forcing MU-MIMO," Freescale Semiconductor Inc., 3GPP TSG RAN WG1, R1-071511, Tech. Rep., 2007. [Online]. Available: http://www.3gpp.com

[7] D. J. Love and R. W. Heath, "Equal gain transmission in multiple-input multiple-output wireless systems," vol. 2, pp. 1124–1128, Nov. 2002.

[8] J. Zhu, J. Liu, X. She, and L. Chen, "Investigation on precoding techniques in E-UTRA and proposed adaptive precoding scheme for MIMO systems," in *14th Asia-Pacific Conference on Communications*, Oct. 2008, pp. 1–5.

[9] D. Tse and P. Viswanath, *Fundamentals of wireless communication*. Cambridge University Press, 2005.

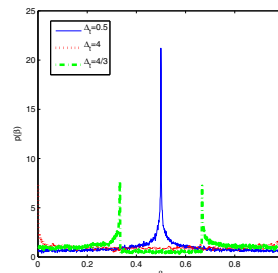[10] A. Gersho and R. M. Gray, *Vector Quantization and Signal Compression*. Kluwer Academic Publishers, 1991.

Fig. 3. The pdf of β when $\Delta_t = 0.5$; $\Delta_t = 4$ and $\Delta_t = \frac{4}{3}$, respectively.
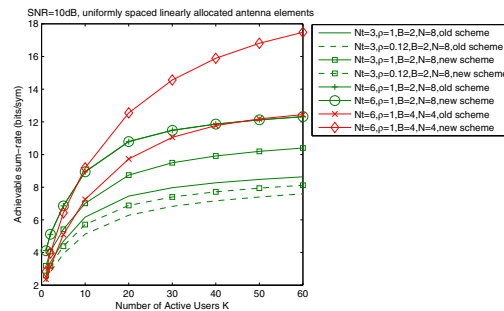

Fig. 4. Comparison of the conventional DFT-based codebook generated from Equation (4) and the proposed improved DFT-based codebook generated by the algorithm summarised in Table I in terms of the achievable sum-rate versus the number of active users K when **1)** $N_t = 3, \rho = 1, B = 2, N = 8$; **2)** $N_t = 3, \rho = 0.12, B = 2, N = 8$; **3)** $N_t = 6, \rho = 1, B = 2, N = 8$ and **4)** $N_t = 6, \rho = 0.12, B = 4, N = 4$.
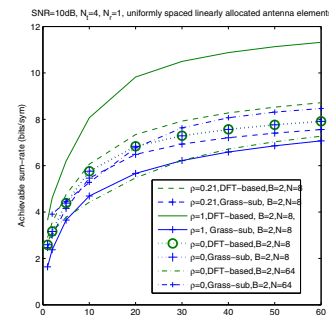

Fig. 5. The achievable sum-rate versus the number of active users K for spatially correlated channels associated with $\rho = 1$, $\rho = 0.21$ and spatially independent channels having $\rho = 0$, when $B = 2$, $N = 8$, and using either the DFT codebook or the Grassmannian subspace packing codebook, respectively.
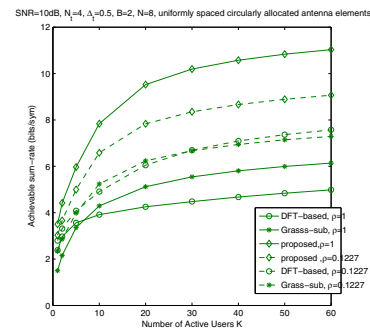

Fig. 6. Comparison of the achievable sum-rate versus the number of active users K using the DFT-based codebook, the Grassmannian subspace packing codebook with $B = 2, N = 8$, as well as the proposed codebook with $B = 2, N = 9$ for spatial correlated channels associated with $\rho = 1$ and $\rho = 0.1227$, respectively, when antenna elements are uniformly spaced and allocated in a circle.